Supporting Information for:

Conformation, Defects and Dynamics of a Discotic Liquid Crystal and Their Influence on Charge Transport

Lucas A. Haverkate[a], *Mohamed Zbiri*[b], *Mark R. Johnson*[b], *Bruno Deme*[b], *Fokko M. Mulder*[a*], *Gordon J. Kearley*[c]

[a]RID, Faculty of Applied Sciences, Delft University of Technology, Mekelweg 15, 2629JB Delft, The Netherlands. [b]Institut Laue Langevin, 38042 Grenoble Cedex 9, France. [c]Bragg institute, Australian Nuclear Science and Technology Organisation, Menai, NSW 2234, Australia.

General properties of the MD simulations

Table S1 summarizes the thermodynamic properties of the 500 ps and 750 ps final MD-simulation runs for TWIST60 and TWIST25, respectively. The average temperature, density and energies of the two runs are very similar.

	$\bar{E}_{tot}$ (kcal mol^{-1})	ΔE_{tot}	$\bar{E}_{pot}$	$\bar{E}_{kin}$	ρ_{av} (g cm^{-3})	T_{av} (K)
TWIST60	460.7	8.0	313.3	147.5	1.07	344
TWIST25	454.7	10.7	309.5	145.3	1.08	338

Table S1. *Thermodynamic properties of the final MD runs*

The average densities are close to the experimental value of 1.06 g cm^{-3} for HAT6D at 345K. The deviation in the total energy, $\Delta E_{tot,}$ within the simulation is less than 2.5% of the average value in both cases, showing that the structures are already in an energy minimum at the start of the final MD runs. Passing from the isolated phase to the condensed phase, the only energy-term that changes

significantly is the non-bond interaction energy. This is shown in Table S2, where all contributions to the potential energy are listed for the isolated molecule and for the bulk-phase TWIST25.

Energy (kcal mol^{-1})	E_{pot}	E_{intern}	E_{nb}	E_{bond}	E_{angle}	$E_{torsion}$	E_{oop}	E_{cross}	E_{LJ}	E_{qq}
1 molecule	430.7	397.6	33.0	55.8	93.9	255.8	1.4	-9.3	27.2	5.9
bulk (TWIST25)	363.7	396.3	-32.6	58.1	92.6	258.3	2.0	-14.7	-36.6	4.0

Table S2 *Internal (E_{intern}) and non-bond (E_{nb}) contributions to the potential energy (E_{pot}) for the isolated molecule and the liquid crystalline phase (TWIST25). The cuttof distance was set at 15 Å.*

The intermolecular interaction-energy is estimated at -67 kcal mol^{-1} (-3.4 eV/molecule) by taking the difference in total potential-energy between isolated and bulk phases. The non-bond energy E_{nb}, composed of the Coulomb (E_{qq}) and Lennard-Jones (E_{LJ}) terms, contributes 98% to this difference. The internal contributions such as the torsion energy hardly change by passing from isolated phase to the bulk, in contrast to earlier observations on HAT5 with a less accurate force-field.[1] Apparently, the redistribution of the dihedral angles of the aliphatic tails due to the columnar packing in the liquid-crystalline phase is not accompanied with significant loss in torsional energy.

Structural properties of the liquid crystalline phase

Orientational order. The orientational order-parameter[1] expresses how well the molecular building-blocks are aligned in a certain direction. In the case of the discotic HAT6 molecules, the order parameter mainly quantifies the alignment of the flat aromatic-cores, since the aliphatic tails are almost evenly distributed above and below the molecular plane (see e.g. Fig. 1b in article). Therefore, we estimated the unit vectors, $\hat{\mathbf{u}}_i$ perpendicular to the molecular plane by only considering the aromatic triphenylene core of each HAT6 molecule. The instantaneous orientional order-parameter is then defined as the largest eigenvalue of the **Q** tensor,

$$Q_{\alpha\beta} = \frac{1}{2N}\sum_{i=1}^{N}(3u_{i\alpha}u_{i\beta} - \delta_{\alpha\beta}) \quad \alpha,\beta = x,y,z \qquad (0.1)$$

with N the total number of HAT6 molecules, 72 in the present case.

After time-averaging over 500 ps we obtained an orientational order-parameter of 0.97 and 0.96 for TWIST25 and TWIST60, respectively. These values lie slightly above the experimental value which ranges from 0.90 to 0.95.[2]

Torsion-angle distribution of the tails. Figure S2 shows the distribution in the 6 torsion angles of the alkyl tails for the columnar phases and the isolated phase. The distributions in the columnar phases TWIST25 and TWIST60 are similar, indicating that the conformation of the alkyl chains is not significantly influenced by the disorder in twist angle and intercolumnar distances. The first two dihedral-angle distributions are fairly broad, the second being more confined to the trans state (180^0). The other four torsion-angles have two well resolved peaks in their distribution function, the higher one corresponding to the trans state and the other to the gauche (60^0). Passing from the isolated to the columnar phase, the trans state of the first, third and fourth dihederal-angle become more occupied.

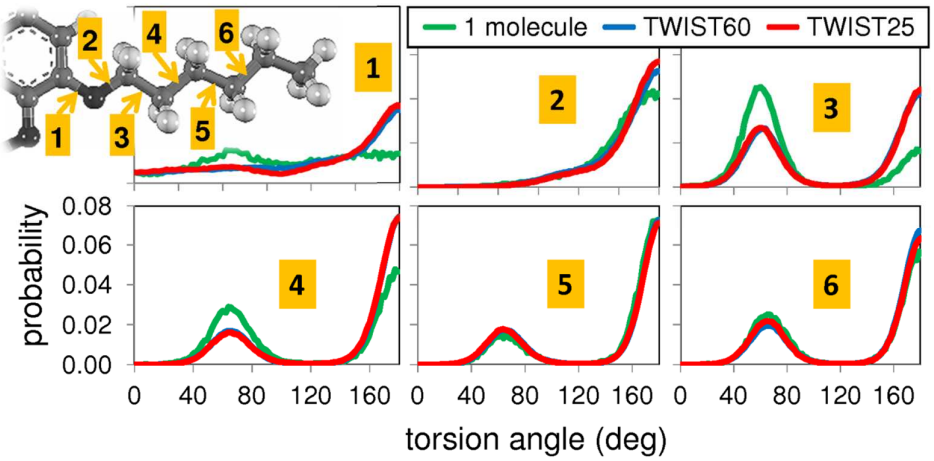

Figure S2 *Torsion angle distribution of the six tail dihedral angles for an isolated molecule (green) and the TWIST25 (red) and TWIST60 (blue) bulk phases.*

This is consistent with the stretching of the tails due to columnar packing and explains why redistribution of the dihedral angles is not accompanied with a significant loss in torsional energy (Table S2).

Dynamic behavior on the picosecond timescale

Figure S3 illustrates the characteristic tilt and twist motions for a single molecule on the 7 ps timescale, showing that these are much more pronounced on this timescale than on the 0.2 ps timescale.

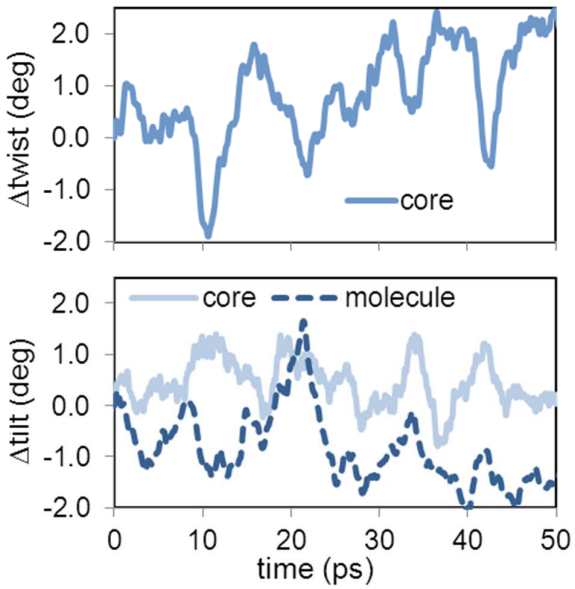

Figure S3 *Picosecond tilt and twist motions for a typical molecule extracted from the TWIST25 trajectory, for both the molecular centre of mass (CM) (broken line) and the movement of the aromatic core CM alone (solid lines)*

Dynamic versus static disorder in core-core distances

The analyses of the QENS data showed that at least a part of the disorder in core-core distances is due to thermal motions on the picosecond timescale. However, the amplitudes of motions seemed too small to fully cover the extend of the asymmetric tail in core-core distances (Figure 6), suggesting that a part of the disorder is static on the picosecond timescale.

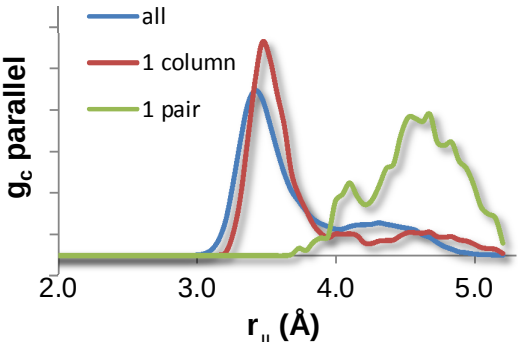

Figure S4 *Parallel intracolumnar correlation function of the aromatic cores, for all columns (blue), one column (brown) and one pair in that column (green), extracted from TWIST25.*

Indeed, Figure S4 shows that the intracolumnar correlation function of the aromatic cores in one column is not the same as that of a single pair in the same column. More specific, within the MD simulation time of 750 ps the core-core distance of the single pair remains within ~3.8 and ~5.3 Å.

The core-core separation of other molecules within the column, on the other hand, mostly remain between ~3 and ~3.8 Å during simulation time. This observation is more generally valid: also for the other columns one part of the molecules have mutual core-core distances fluctuating around the minimum energy separation, while the other part remains 'trapped' with core-core distances larger than ~3.8 Å. One of the 72 HAT6 molecules actually showed a transition from the large distance tail of the distribution towards the typical peak around 3.4 Å. There is thus a clear distinction between relatively small picosecond timescale motions of the aromatic cores and the much slower dynamics involved in the continuous redistribution of 'structural traps' for charge transport. The picosecond motions are observed by QENS and interfere with the charge transfer between molecules, while the structural traps appear to be static for charge hopping.[3]

Reference List

1. Cinacchi, G.; Colle, R.; Tani, A. *J. Phys. Chem. B* **2004,** *108*, 7969-7977.
2. Goldfarb, D.; Luz, Z.; Zimmermann, H. *J. Phys.* **1981,** *42*, 1303-1311.
3. Troisi, A.; Cheung, D. L.; Andrienko, D. *Phys. Rev. Lett.* **2009,** 116602 .